Received: 16 April 2020 | Revised: 29 May 2020 | Accepted: 5 June 2020

DOI: 10.1002/jhet.4060

WILEY

ARTICLE

Identification of novel thiourea-stilbene-triazine conjugates as persuasive lymphoid tyrosine phosphatase inhibitors

Iram Batool[1] | **Farukh Jabeen**[1] | **Nadeem Ahmed Vellore**[2] | **Ghulam Shabir**[1] | **Aamer Saeed**[1]

[1]Department of Chemistry, Quaid-i-Azam University, Islamabad, Pakistan

[2]Huntsman Cancer Institute, University of Utah, Salt Lake City, Utah

Correspondence
Prof Dr Aamer Saeed Department of Chemistry, Quaid-i-Azam University, Islamabad, 45320, Pakistan.
Email: asaeed@qau.edu.pk

Present address
Farukh Jabeen, Department of Chemistry and Biochemistry Laurentian University, 935 Ramsey Lake Road, Sudbury, ON, P3E 2C6, Canada

Funding information
University of Utah, College of Pharmacy

Abstract

A library of novel thiourea-based symmetrical stilbene-triazines (**5a-i**) was synthesized in an effort to develop new protein tyrosine phosphatase LYP inhibitors. The versatile nature of 2,4,6-trichloro-1,3,5-triazine allows considerable scope for derivatization and hence exploration of structure activity relationships. A convenient and versatile three-step synthetic approach involved the successive replacement of the two chloro groups of 2,4,6-trichloro-1,3,5-triazine by a variety of substituents for structural modification. The newly synthesized derivatives were subjected to tyrosine phosphatase LYP inhibition studies. The results for the in vitro bioassays were promising with the identification of compound **5k** and **5l** having a 4-methyl and 4-methoxy substituent on phenyl ring, as the lead and selective candidate for LYP inhibition with an IC_{50} value of 2.1 ± 0.05 μM and 28 ± 3.3 μM, respectively. Moreover, docking studies were carried out to determine the possible interaction sites of thiourea-based stilbene-triazine compounds with Lymphoid Tyrosine Phosphatase. Results of docking computations further ascertained the inhibitory potential of compound **5k** and **5l**. The results indicated that the compound **5k** may serve as a structural model for the design of most potent LYP inhibitors.

1 | INTRODUCTION

Fluorescent brightening agents (FBAs) are dyes that absorb light in the UV and violet region (340-370 nm) of the electromagnetic spectrum and re-emit light in the blue region (typically 420-470 nm). These include five or six membered heterocycles such as imidazolines, diazoles, triazoles, benzoxazolines, coumarins, naphthalimides, pyrazines, and triazines.[1,2] Stilbenes especially diphenyl stilbenes are the most common structural motif used in these compounds. The extensive pi-systems of these compounds are associated with the closely spaced electronic energy levels that allow for energy transitions within the visible range (eg, n-pi transitions).[2] Moreover, 1,3,5-triazine derivatives have been found to exhibit the variety of biological applications such as an antioxidant,[2] protein kinase CK2 inhibition,[3] anti-inflammatory,[4] antimicrobial,[5] hedgehog signaling pathway inhibition.[6] Heterobicyclic nitrogen systems bearing a 1,2,4-triazine moiety,[7] 6-substituted-2-b-galactosyl-1,2,4-triazine,[8] and 2,4-diamino-1,3,5-triazine derivatives[9] have been reported as potent anticancer inhibitors.

Triazine-stilbene hybrids are one of the important classes of FBAs and are effective for attaining high degrees of whiteness on polyamide-6.[10] These have been used as textile auxiliaries or in detergents.[11] The charge-transfer complexes were also obtained by the interaction between symmetrically substituted stilbene-triazine derivatives with chloranilic acid. Stilbene-triazine derivatives comprising the polymerizable groups have been used for radical polymerization of styrene. The photophysical and photochemical characteristics in aqueous and ethanol solution of

some stilbene-triazine fluorescent brighteners containing 2-hydroxyethylamino groups and their trans-cis isomers in equilibrium have been studied.[12,13] The cytotoxic activity of some stilbene-triazine derivatives containing amino acid groups has also been reported.[14]

The reversible phosphorylation of tyrosine residues play a key role in regulating numerous cellular functions including cell division, gene transcription, transport of materials across the cell membrane, cellular adhesion, and activation of the immune response.[15] Control of tyrosine phosphorylation is maintained through protein tyrosine kinases (PTKs) and protein tyrosine phosphatases (PTPs) enzymes. These two enzyme classes operate in opposition of each other, and the delicate balance of their activity gives the cell control of the associated pathways. Disruption of this activity can impair cell function and lead to a variety of negative consequences.

The PTP lymphoid tyrosine phosphatase (LYP) is a 105 kDa enzyme found in lymphocytes, where it functions as a negative regulator in T cell receptor (TCR) signaling through dephosphorylation of the kinases Lck, Fyn, and Zap-70, resulting in reduced T cell activation.[16 Two single nucleotide polymorphism (SNP) mutations found in LYP are of therapeutic interest as they have been shown to be associated with changes in disease risk. The SNP G778A produces the R263Q mutant, which leads to a catalytic site restructuring that is believed to be the cause of an observed reduction in enzymatic activity found with this mutant.[17] R263Q has been associated with a reduced risk for several diseases, including rheumatoid arthritis,[18] systemic lupus erythematosus,[17] and ulcerative colitis.[19] The SNP C1858T results in a R620W mutation, which occurs in a region responsible for binding to Csk,[20] a tyrosine kinase, which also acts as a negative regulator of TCR signaling.[21] It is currently believed that R620W results in increased TCR signaling suppression through a gain-of-function, but the impact this mutation has on LYP activity and the mechanism by which it functions is currently unclear.[22] In contrast to the R263Q, R620W has been implicated in an increased prevalence of a number of diseases including type 1 diabetes,[20] rheumatoid arthritis,[23] systemic lupus erythematosus,[24] Graves' disease, and others.[25–27]

The apparent relationship between LYP activity and disease risk suggests that LYP may be a valuable drug target for inhibitor development. Over the past few five years, a number of LYP inhibitors have been reported in the literature. He et al. reported on the discovery of a salicylic acid based inhibitor (A) showing both excellent potency and selectivity. The compound was found to have an IC_{50} value of 0.259 μM against LYP and over 9-fold specificity against other PTPs.[28] Both bone marrow derived mast cells and mouse models showed that (A) inhibited the granulation of mast cells, suggesting that it has in vivo efficacy. The discovery that this compound was found to bind to both the catalytic site as well as several nearby pockets was cited as the reason for its effectiveness. Stanford et al. described a non-competitive inhibitor (B) which does not use a phosphomimetic in its structure.[29] Mapping studies suggested a mechanism of inhibition in which (B) binds to an allosteric binding pocket rather than the catalytic site. This was supported by experiments, which showed that both **B** and **C** a known catalytic site inhibitor could induce inhibition simultaneously. The molecule was found to have moderate potency (IC_{50} = 5.28 μM) and cell permeability, but only showed selectivity towards HePTP. Kulkarni et al identified several LYP inhibitors from the Spectrum Collection, a compound library containing 2000 chemicals.[30] In addition to a number of known PTP inhibitors, several new inhibitors were identified, including epigallocatechin 3,5-digallate (EGCDG), which was found to be very potent against LYP (IC_{50} = 50 nM) and selectivity against CD45 but not PTP-PEST. Incubation at 500 nM with Jurkat T cells resulted in increased Zap-70 phoare potentssphorylation, suggesting that EGCDG can inhibit LYP in vivo. On the other hand, various triazine derivatives have been reported as potent inhibitors of P13K; sulfonyl stilbene derivatives are HIV inhibitors whilst the bisthioureas are NNRT inhibitors (Figure 1).

Thus, design and synthesis of new molecules incorporating all the three bioactive components in a single structural unit leading to a new series of C-2 symmetric novel molecules as a new entry to potent and selective LYP inhibitors was intended (Scheme 2).Using an in vitro-LYP activity assay, these compounds were tested for their efficacy in inhibiting LYP and the potential of this scaffold as future inhibitors development is discussed.

2 | RESULTS AND DISCUSSION

2.1 | Synthesis of thiourea-based stilbene-triazine derivatives (5a-l)

The new thiourea-based stilbene-triazine derivatives were prepared by multistep synthetic pathway as described in Scheme 1. Synthesis was achieved by reacting 2,4,6-trichloro-1,3,5-triazine with separately synthesized thioureas (**2a-l**). This reaction resulted in the formation of dichlorotriazinyl intermediates (**3a-l**), which were then condensed with diaminostilbene disulfonic acid (**4**) to afford *bis*-monochlorotriazines (**5a-l**) in good yields. The maintenance of low temperature and pH was found to be most critical for the successful coupling of 2,4,6-trichloro-1,3,5-triazine with thioureas. The newly synthesized molecules contain bisthiourea, stilbene sulfonic acid, and

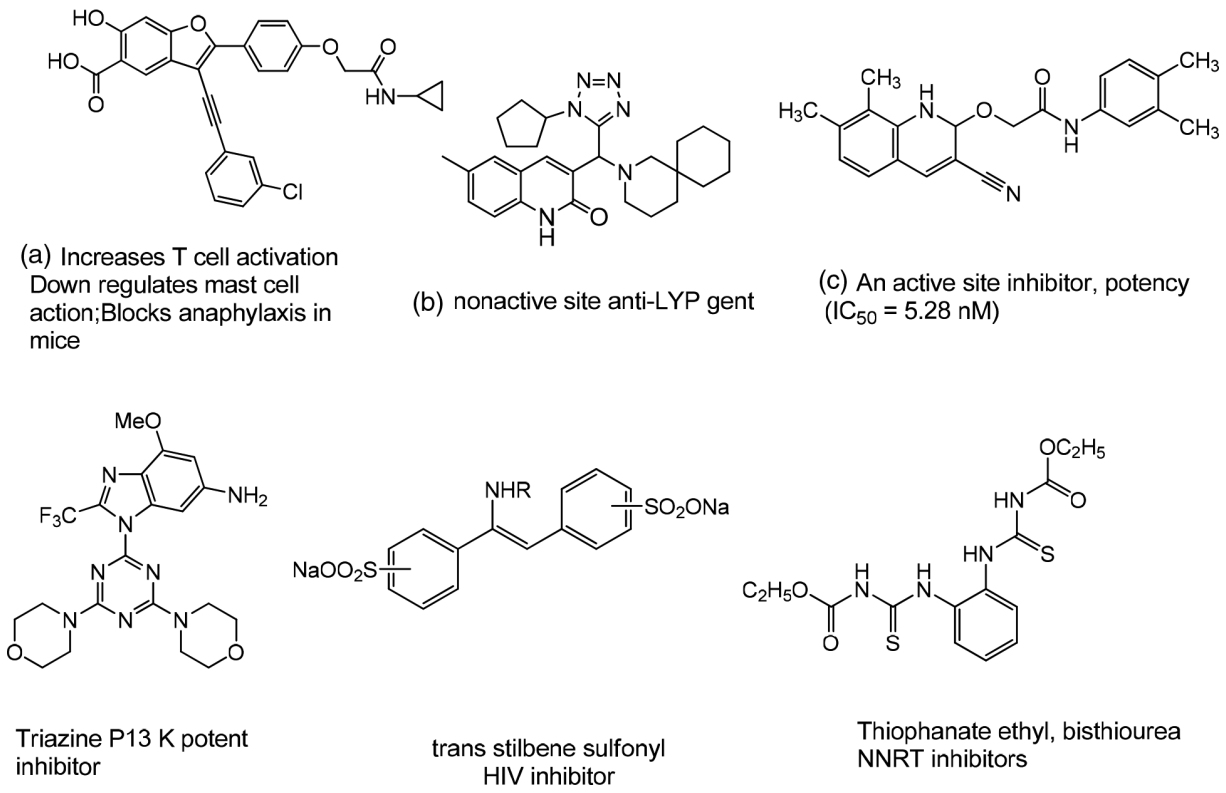

FIGURE 1 Some lead inhibitors of (LYP) and bioactive triazines, stilbenes, and bis-thioureas

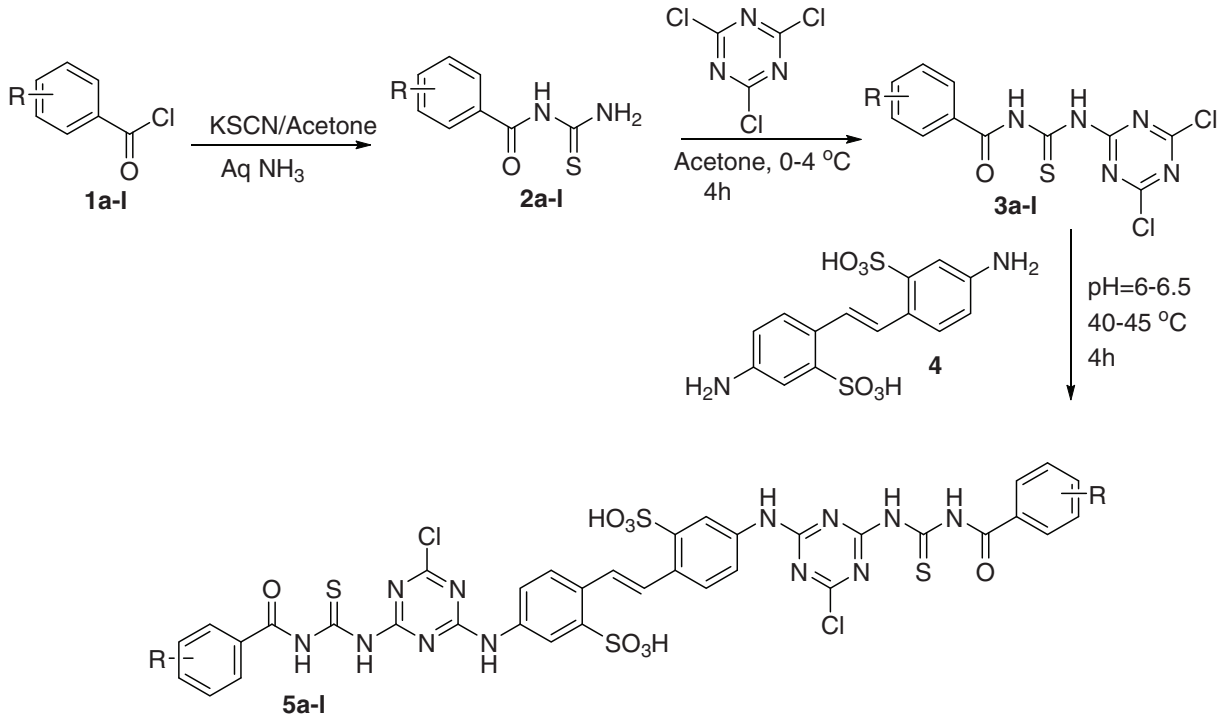

SCHEME 1 Synthesis of thiourea-based stilbene-triazine derivatives (**5a-l**)

triazine scaffolds in a single structural unit. Table 1 lists the variety of substituents attached to phenyl ring of these symmetrical molecules.

FTIR analysis data of compounds **5a-l** showed the peaks in the range of 3372 to 3465 cm^{-1} due to the stretching vibrations of NH groups and the characteristic

TABLE 1 Substituents attached to phenyl ring of hybrid molecules (**3a-l)** and (**5a-5L**) and their percentage yields

Compound	*R*	Yield (%)	Compound	*R*	Yield (%)
3a	H	81	**5a**	H	68
3b	2-OH,3,4-diNO_2	75	**5b**	2-OH,3,4-diNO_2	71
3c	3,4,5-tri-OCH_3	69	**5c**	3,4,5-tri-OCH_3	65
3d	2-F,3-OCH_3,4-Br	70	**5d**	2-F,3-OCH_3,4-Br	75
3e	3,5-diOH	73	**5e**	3,5-diOH	70
3f	2-Br	78	**5f**	2-Br	67
3g	2-CH_3	79	**5g**	2-CH_3	69
3h	2-OH	79	**5h**	2-OH	72
3i	2-NO_2	77	**5i**	2-NO_2	78
3j	4-NO_2	78	**5j**	4-NO_2	58
3k	4-CH_3	74	**5 k**	4-CH_3	79
3l	4-OCH_3	72	**5l**	4-OCH_3	67

peaks for S═O and C═O were observed in the range of 1035 to 1098 cm^{-1} and 1703 to 1714 cm^{-1}, respectively. In ^{1}H NMR spectra, characteristic broad signal appeared at δ 11.22 to 11.39 ppm indicating the presence of NH protons and the signals for aromatic and olefinic protons appeared in the range of δ 6.44 to 8.39 ppm. ^{13}C NMR spectral data showed the most deshielded carbon at δ 179.62 to 175.71 ppm assigned to C═S, whereas C═O carbon resonated in the range of δ 167.89 to 168.81 ppm. Signals appearing at δ 126.23 to 126.63 ppm were assigned to olefinic carbons, while those in the range δ 112.25 to 151.89 ppm correspond to aromatic carbon atoms (Supporting Figures S1-S16).

2.2 | LYP inhibition screening

Dephosphorylation of the compound 6,8-difluoro-4-methylumbelliferyl phosphate (DiFMUP) to the fluorophoric molecule 6,8-difluoro-4-methylumbelliferyl (DiFMU) is an established PTP activity assay.[31] Compound inhibition effectiveness was determined by measuring the extent of dephosphorylation of DiFMUP by LYP. The synthesized compounds were initially screened at a concentration of 100 μM. Of the twelve synthesized compounds, **5b**, and **5c** were found to be only partially soluble in DMSO at the required concentrations and were thus excluded from testing. Additionally, compounds **5g** and **5i** were found to have reached maximum fluorescence at the first read, preventing determination of inhibition values for these compounds. Results of the initial screening are presented in bar graph shown in Figure 2. The figure shows the percentage inhibition at ordinate (y-axis), while **abscissa** shows the compounds tested.

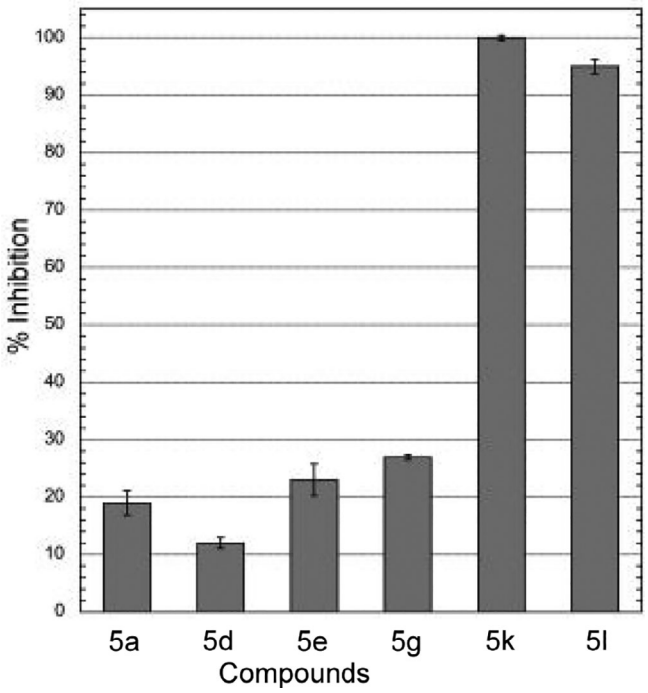

FIGURE 2 Percent inhibition of LYP activity by synthesized compounds in the initial screen. Compounds were tested at a concentration of 100 μM

Compounds **5k** and **5l** showed potent inhibition with reductions of 100% and 95.3% in LYP activity, respectively. Interestingly compound **5g**, which contains a methyl group in the 2 positions as opposed to the 4 position as seen in compound **5k**, showed a much smaller percent inhibition, suggesting that a substituent in the 4 position plays a critical role in the function of the molecule. Both compounds **5k** and **5l** contain non-charged substituents (methyl and methoxide), but due to the fact

that the nitro containing compound **5j** could not be successfully tested it is unknown if or how formal charge at the 4 position would impact inhibition.

Compounds **5k** and **5l** showed IC_{50} values below 100 μM and were selected for IC_{50} testing. IC_{50} curves for these compounds are shown in Figure 3. Compound **5k** and **5l** are the most active compounds of the series, they showed good inhibition potential and were selected for the IC_{50} testing. Compound **5k** found to be most potent agent pf the series followed by compound **5l**. The IC_{50} value for **5l** was calculated to be 28 ± 3.3 μM, while compound **5k** was found to be over 13 times more potent with an IC_{50} value of 2.1 ± 0.05 μM. To further understand the binding interaction of these compounds, we used computational docking of compounds to LYP protein. In particular, both compound **5k** and **5l** were found to interact favorably with LYP protein with a docking score of −9.5 and 10.2 kcal/mol (Scheme 2).

Based on the initial assessment of the binding pose, we found that the sulfonate group docked at the P-loop in all the cases providing as an anchoring point for the flanking regions to interact with the protein (Figure 4). It is also interesting to note that both compounds occupied the adjacent binding site (LYP insert loop), while forming a cation-pi interaction with K39 residue (of the LYP-insert loop) and the terminal phenyl group of the compound. While, the other end of the compound showed differential binding interaction. The compound **5k** showed favorable contacts with the conserved WPD loop while compound **5l** interacted with β3 loop. Interestingly, other compounds, such as **5a**, **5d**, **5e** and **5g** also showed favorable docking score with the LYP protein.

Figure **5**A,B represents the docking pose of ligand 5l inside the active site of LYP in tri and di dimensional space, respectively. The active site is surrounded by the key amino acid residues including, Lys32, Ser35, Lys39, Tyr44, Thr46, Asp62, Ile63, Tyr66, Cys129, Met130, Tyr132, Glu133, Met134, Lys191, Asn192, Trp193, Ser227, Ser228, Ala229, Gly230, Cys231, Gly232, Arg233, Thr234, Arg266, Ser271, Pro270, Gln274, Thr275, Glu277, Gly278. In our docking model, the carbonyl oxygen in ligands 5l made close contact with the active site through copious strong hydrophobic and hydrophilic interactions. The enhanced affinity of ligand 5l towards the residues was reflected by their strong interaction with residues such as Lys32, Lys39, Asp62, Asn192, Ser227, Ser228, Ala229, Arg233, Ser271, Gly278. Besides being directly involved in the architecture of the active site, the residue plays a vital role in positioning other key residues in the active site appropriately for the catalysis. These residues established strong interaction with each other through hydrogen binding, van der Waals and other hydrophobic and polar interactions. Residues are aligned around the active site and are available to interact with the ligand due to these interactions.

The docking model represents that compounds ligand 5l showed a distinct orientation for interacting with the active site residues LYP. The ligands anchored in active site through determinant hydrogen bonding, where all the three atoms of sulphur trioxide attached to the phenyl ring of left half of the stilbene molecule showed the most interesting pattern in anchoring the molecule inside the active site by establishing 10 strong hydrogen bonding with Ser228, Ala229, Lys230, Ser227, Cys231, Arg233 as

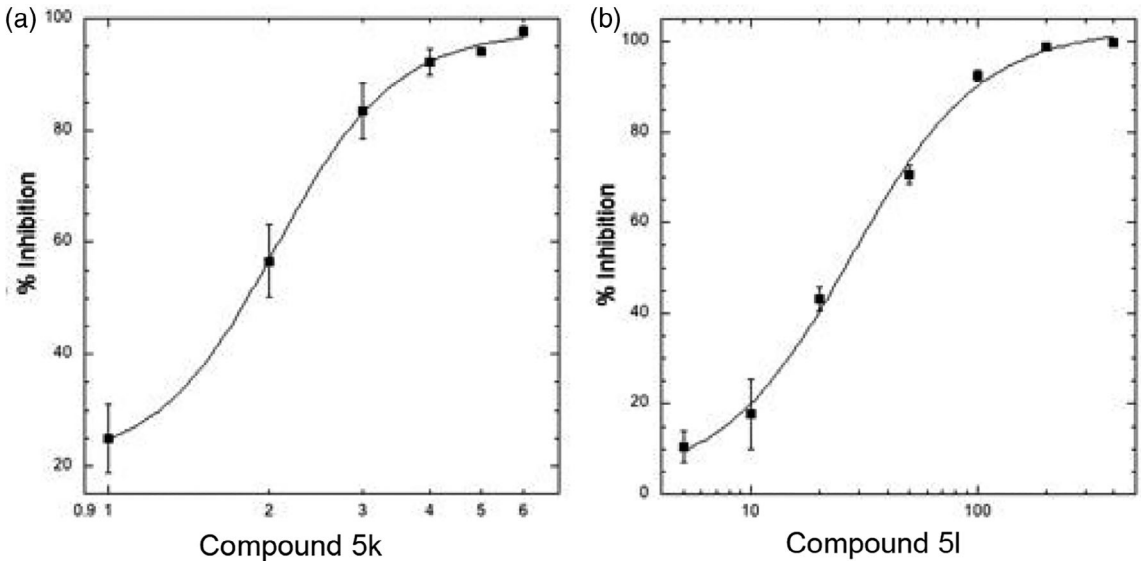

FIGURE 3 IC_{50} curves for compounds, A, **5k** and, B, **5 L**. The abscissa shows the concentration of the compound 5 k and 5 L in μM, while ordinate represent the percentage inhibition. The IC_{50} values were calculated to be 2.1 ± 0.05 μM and 28 ± 3.3 μM, respectively

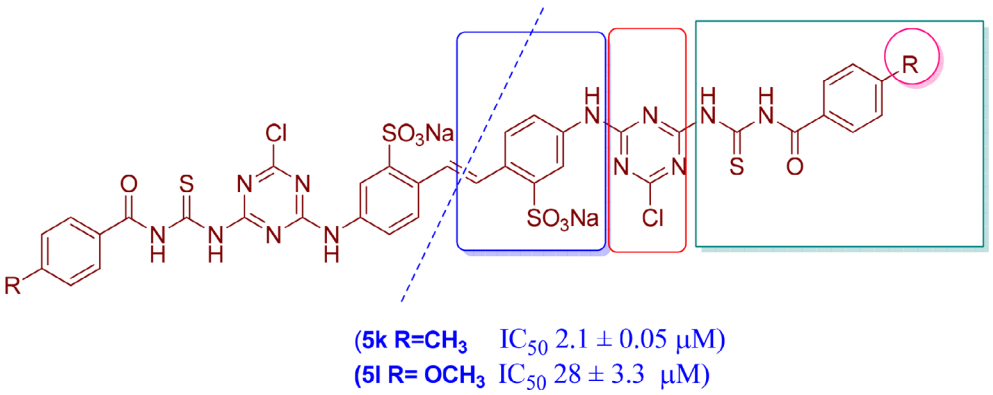

SCHEME 2 Structural architecture of C-2 symmetrical molecules and effect of substituent on activity

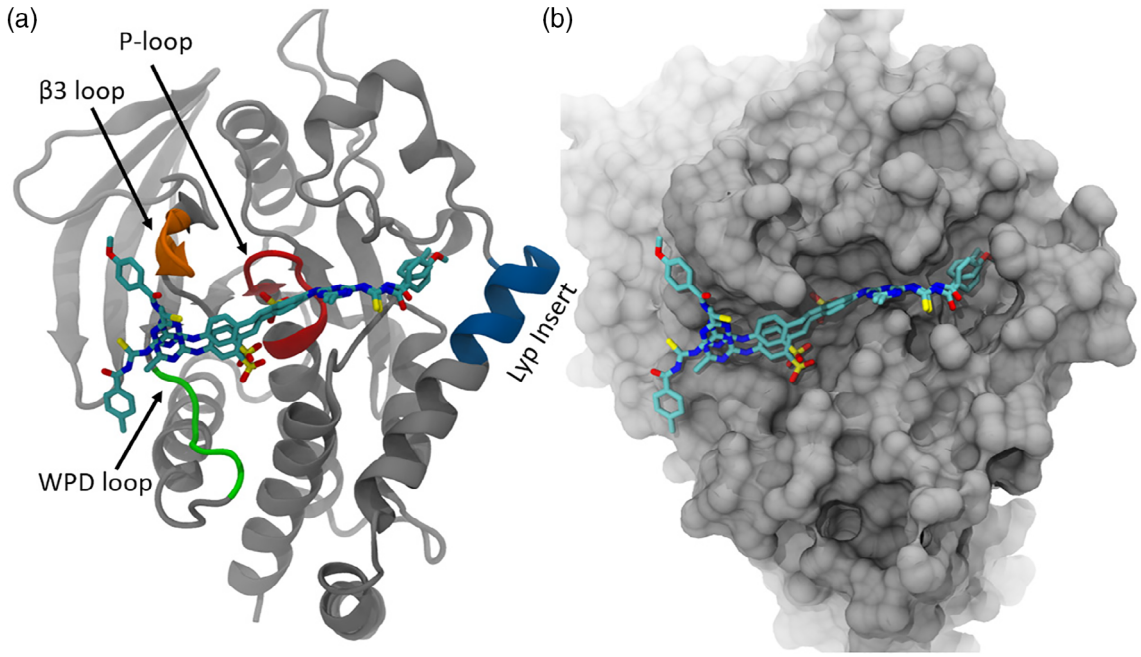

FIGURE 4 Modeling of thiourea-based stilbene-triazine derivatives on LYP protein. Docked conformation of compound **5k** and **5 l** are overlaid on LYP protein. The protein is represented using, A, secondary structure (with P-loop (red), Lyp-insert (blue), β3-loop (orange), and WPD loop (green) highlighted) and, B, using the van der Waals surface

shown in Figure 5A,B. This part of the molecule got privileged to be strengthen inside the active site by establishing further hydrogen bonding through both the amine of thiourea and carbonyl oxygen with Asp62, Lys32, Ser271, respectively, in addition to three strong aromatic hydrogen bonding (Figure 4A) with the Lys39, and Asp62 by terminal Phenyl ring, which consequently provided the strong binding to the entire left half of the molecule. The flanking region made close contacts by establishing the π-π and π-H interactions with Arg233 as shown in Figure 5A,B. Moreover, a hydrogen bonding of amine of thiourea of the flanking region (right half of the molecule) architected a hydrogen bonding with Asn192, as displayed in Figure 5A,B, a well required contact, playing a significant role in anchoring the flanking part of the molecule inside the active site gorge.

Figure 5B displays the interaction of the ligand with amino acid residues in active site in two dimensional space. Polar amino acids are shown in pink color circle, while amino acids basic in character are shown in blue color. Lipophilic amino acids are shown in green color. Interactions are shown in dotted lines in Figure 5A while interactions are shown in both solid and dashed lines in Figure 5B. Hydrogen bonding is shown in red color dashed lines, Figure 5A, depicting the orientation of molecule in three dimensions. The direction of the arrow shows the donor and acceptor (points toward acceptor). Aren-aren and aren-H interactions are shown in green

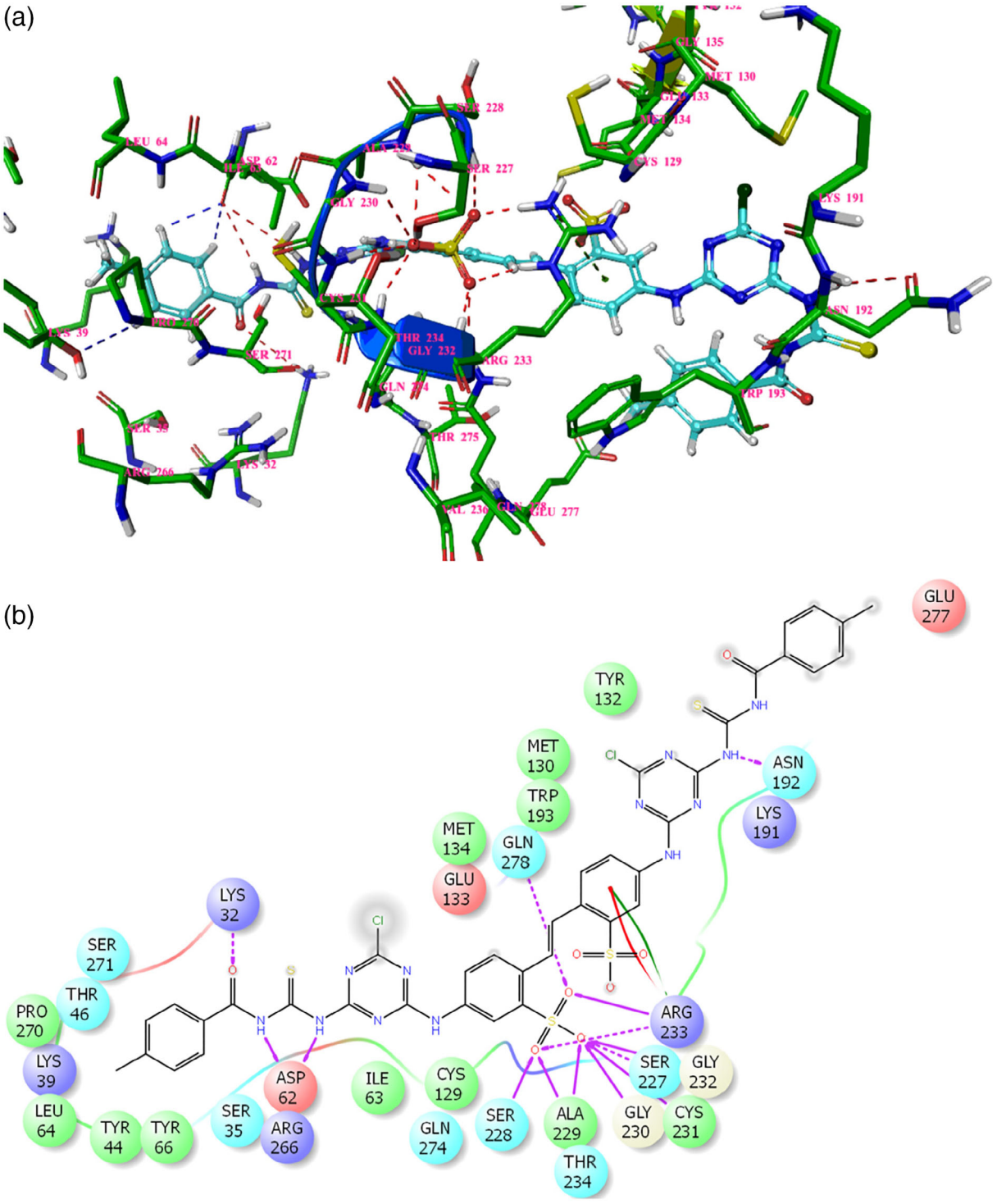

FIGURE 5 Binding mode of compounds **5k** inside the active site of LYP. A, Docking poses of compound **5k** in 3D space. Ligands are shown in ball n stick mode in elemental and cyan color and key residues are shown by stick mode, elemental color, and green color, respectively. Hydrogen bonding of ligand atoms with residue atoms is shown in red dashed lines. Aromatic hydrogen bonding is shown in blue colored dashed lines. π -cation interactions are represented by green dashed lines. A, Docking pose of compound **5k** inside the active site in 2 dimensional space

and red solid lines in 2D image (Figure 5B) while these are shown in green colored dashed lines and cyan colored dashed lines in tri dimensional space (Figure 5A).

Although docking simulation were useful in understanding the interaction of these compounds on LYP protein; however it was not helpful in explaining some of

the differences in the binding observed experimentally. This is due to the fact that these compound exhibit large molecular size with too many rotatable bonds, which often present challenges in accurate sampling and scoring of the poses. In future studies, we would incorporate molecular simulation to understand the induced effect, these flanking region of the compound exerts on the LYP protein. Additionally, the exact mechanism by which the methoxide reduces inhibitor efficiency will likely play a key role in optimizing future inhibitors in this molecule class.

3 | EXPERIMENTAL

3.1 | General procedure for the synthesis of stilbene-triazine derivatives (5a-l)

To a well stirred acetone (10 mL) in round bottomed flask (50 mL) was added cyanuric chloride (**1**, 0.38 g, 0.002 mol) at 4°C to 5°C in an ice bath. To this suspension was added an acetone solution (10 mL) of separately synthesized thioureas **2a-l** (0.002 mol) and stirred the reaction mixture at temperature 4°C to 5°C for 4 hours until completion of reaction was observed from TLC (PE: EA, 4:1). The reaction mixture was allowed to stand at room temperature for 1 hour, which resulted in settling down of precipitates of intermediates **3a-l** which were dried at room temperature in the folds of filter paper and calculated their yields.

The compounds **3a** (0.001 mol) was suspended in distilled water (10 mL) at room temperature in 50 mL round bottomed flask and started stirring the reaction mixture. The aqueous solution (10 mL) of 4,4-diaminostilbenedisulfonic acid (**4**) (0.0005 mol) was added to the above mixture. The temperature was gradually increased to 40 to 45°C and continued stirring the reaction at this temperature by maintaining pH 6 to 6.5 with HCl. The reaction mixture was stirred for 4 hours until completion of reaction was observed from TLC (Chloroform: Methanol, 9:1). In this way *bis*-monochlorotriazinyl derivatives **5a** was synthesized. The other derivatives of *bis*-monochlorotriazine **5b-l** were accomplished by using thiourea derivatives **3b-l**. The characteristic spectroscopic data of synthesized compounds **5a-l** and intermediate thioureas **3a-l** is as follows.

3.2 | Benzoic acid derivative of triazine (3a)

Mol.Wt: 326.9; Light yellow solid, R_f 0.31 FTIR: 3427 (N—H), 1712 (C═O), 1596 (C═N), 1038 (S═O), 658 (C—Cl), 595 (C—Br) cm^{-1}; ^1H NMR (300 MHz, DMSO-d_6): δ 11.25 (br s, 2H, N*H*), 7.99-7.93 (m, 2H), 7.53-7.45 (m, 2H), 7.31 (tt, J = 7.5, 2.0 Hz, 1H). ^{13}C NMR (75 MHz, DMSO-d_6): δ 179.62 (C═S), 167.10 (C═O), 165.75 (C—Cl), 163.15(C═N), 134.34-128.10 (Ar—*C*). Anal. Calcd for $C_{11}H_7Cl_2N_5OS$: C, 40.26; H, 2.15; N, 21.34; S, 9.77. Found: C, 40.20; H, 2.22; N, 21.23; S, 9.85. EIMS calculated for $C_{11}H_7Cl_2N_5OS$ ($M^{+\bullet}$) 327.

2-Hydroxy-3,4-dinitrobenzoic acid derivative of triazine (3b).

Mol.Wt: 433; Yellow solid, R_f 0.31; FTIR: 3520 (O—H), 3437 (N—H), 1705 (C═O), 1603 (C═N),1455 (NO_2), 1059 (S═O), 650 (C—Cl) cm^{-1}; ^1H NMR (300 MHz, DMSO-d_6): δ 11.22 (br s, 2H, N*H*), 8.27 (d, J = 7.5 Hz, 1H), 7.80 (d, J = 7.5 Hz, 1H). ^{13}C NMR (75 MHz, DMSO-d_6): δ 177.65 (C═S), 168.25 (C═O), 167.93(C—Cl), 163.15 (C═N), 160.91(C—OH), 144.07(C-NO_2), 131.76-119.79 (Ar—*C*).Anal. Calcd for $C_{11}H_5Cl_2N_7O_6S$: C, 30.43; H, 1.16; N, 22.58; S, 7.38. Found: C, 30.36; H, 1.22; N, 22.51; S, 7.43. EIMS calculated for $C_{11}H_5Cl_2N_7O_6S$ ($M^{+\bullet}$) 433.

3,4,5-Trimethoxybenzoic acid derivative of triazine (3c).

Mol.Wt: 417; Light yellow solid, R_f 0.40; FTIR: 3422 (N—H), 1708 (C═O), 1599 (C═N), 1110 (C—O), 1073 (S═O), 658 (C—Cl) cm^{-1}; ^1H NMR (300 MHz, DMSO-d_6): δ 11.24 (br s, 2H, N*H*), 7.22 (s, 2H), 3.90 (s, 6H), 3.84 (s, 3H). ^{13}C NMR (75 MHz, DMSO-d_6): δ 178.62 (C═S), 169.13 (C═O), 166.96 (C—Cl), 163.15(C═N), 151.96 (C—O), 140.07-107.41 (Ar—C), 60.68 (O-CH_3), 56.26 (O-CH_3). Anal. Calcd for $C_{14}H_{13}Cl_2N_5O_4S$: C, 40.20; H, 3.13; N, 16.74; S, 7.67. Found: C, 40.12; H, 3.20; N, 16.70; S, 7.74.EIMS calculated for $C_{14}H_{13}Cl_2N_5O_4S$ ($M^{+\bullet}$) 417.

2-Flouro-3-methoxy-4-bromobenzoic acid derivative of triazine (3d).

Mol.Wt: 453; Light yellow solid, R_f 0.36 FTIR: 3445 (N—H), 1710 (C═O), 1601 (C═N), 1234 (C—F), 1115 (C—O), 1072 (S═O), 652 (C—Cl) cm^{-1}; ^1H NMR (300 MHz, DMSO-d_6): δ 11.29 (br s, 2H, N*H*), 7.69 (d, J = 7.5 Hz, 1H), 7.38 (d, J = 7.5 Hz, 1H), 3.94 (s, 3H). ^{13}C NMR (75 MHz, DMSO-d_6): δ 177.87 (C═S), 168.22 (C═O), 166.22 (C—Cl), 166.16 (C—F), 163.15 (C═N), 154.00-116.91 (Ar-*C*), 60.80 (O-CH_3).Anal. Calcd for $C_{12}H_7BrCl_2FN_5O_2S$:C, 31.67; H, 1.55; N, 15.39; S, 7.04. Found:C, 31.62; H, 1.61; N, 15.30; S, 7.14. EIMS calculated for $C_{12}H_7BrCl_2FN_5O_2S$ ($M^{+\bullet}$) 453.

3,5-Dihydroxybenzoic acid derivative of stilbene-triazine (3e).

Mol.Wt: 359; Light yellow solid, R_f 0.29; FTIR: 3510 (O—H), 3395 (N—H), 1716 (C═O), 1602 (C═N), 1108 (C—O), 1070 (S═O), 654 (C—Cl) cm^{-1}; ^1H NMR (300 MHz, DMSO-d_6): δ 11.27 (br s, 2H, N*H*), 6.84 (s, 2H), 6.57 (s, 2H), 6.48 (s, 1H). ^{13}C NMR (75 MHz, DMSO-

d_6): δ 178.85 (C═S), 168.17 (C═O), 166.96 (C—Cl), 163.74 (C═N), 158.46-105.87 (Ar-*C*). Anal. Calcd for $C_{11}H_7Cl_2N_5O_3S$: C, 36.68; H, 1.96; N, 19.45; S, 8.90. Found: C, 36.64; H, 1.99; N, 19.40; S, 8.98.EIMS calculated for $C_{11}H_7Cl_2N_5O_3S$ ($M^{+\bullet}$) 359.

2-Bromobenzoic acid derivative of triazine (3f).

Mol.Wt: 405; Light yellow solid, R_f 0.33 FTIR: 3429 (N-H), 1711 (C═O), 1590 (C═N), 1078 (S═O), 648 (C—Cl), 593 (C—Br) cm^{-1}; ^1H NMR (300 MHz, DMSO-d_6): δ 11.28 (br s, 2H, N*H*), 7.82 (dd, *J* = 7.4, 2.1 Hz, 1H), 7.72 (dd, *J* = 7.4, 2.1 Hz, 1H), 7.39 (td, *J* = 7.5, 2.1 Hz, 1H), 7.33 (td, *J* = 7.5, 2.0 Hz, 1H).^{13}C NMR (75 MHz, DMSO-d_6): δ 177.59 (C═S), 168.20 (C═O), 166.30 (C—Cl), 164.35 (C═N), 137.17-118.58 (Ar—*C*). Anal. Calcd for $C_{11}H_6BrCl_2N_5OS$: C, 32.46; H, 1.49; N, 17.20; S, 7.88. Found: C, 32.43; H, 1.53; N, 17.14; S, 7.95.EIMS calculated for $C_{11}H_6BrCl_2N_5OS$ ($M^{+\bullet}$) 405.

2-Methylbenzoic acid derivative of triazine (3g).

Mol.Wt: 341; Light yellow solid, R_f 0.38 FTIR: 3411 (N—H), 1705 (C═O), 1595 (C═N), 1440 (C—H), 1055 (S═O), 662 (C—Cl) cm^{-1}; ^1H NMR (300 MHz, DMSO-d_6): δ 11.22 (br s, 2H, N*H*), 7.56 (dd, *J* = 7.2, 2.2 Hz, 1H), 7.51-7.44 (m, 1H), 7.38 (dd, *J* = 8.2, 6.3 Hz, 2H), 2.39 (d, *J* = 1.0 Hz, 3H). ^{13}C NMR (75 MHz, DMSO-d_6): δ 177.47 (C═S), 168.15 (C═O), 167.99 (C—Cl), 162.27(C═N), 137.76-127.02 (Ar—*C*), 19.98 (CH_3). Anal. Calcd for $C_{12}H_9Cl_2N_5OS$: C, 42.12; H, 2.65; N, 20.47; S, 9.37. Found: C, 42.06; H, 2.69; N, 20.44; S, 9.40.EIMS calculated for $C_{12}H_9Cl_2N_5OS$ ($M^{+\bullet}$) 341.

2-Hydroxybenzoic acid derivative of triazine (3h).

Mol.Wt: 343; Light yellow solid, R_f 0.33; FTIR: 3505 (O—H), 3370 (N—H), 1710 (C═O), 1610 (C═N), 1105 (C—O), 1072 (S═O), 656 (C—Cl) cm^{-1}; ^1H NMR (300 MHz, DMSO-d_6): δ 11.30 (br s, 2H, N*H*), 7.73 (dd, *J* = 7.5, 2.0 Hz, 1H), 7.43 (td, *J* = 7.5, 2.0 Hz, 1H), 7.04 (dd, *J* = 7.4, 2.1 Hz, 1H), 6.93 (td, *J* = 7.5, 2.0 Hz, 1H), 5.73 (s, 1H). ^{13}C NMR (75 MHz, DMSO-d_6): δ 178.76 (C═S), 168.29 (C═O), 167.96 (C-Cl), 163.15 (C═N), 159.59-117.18 (Ar-*C*). Anal. Calcd for $C_{11}H_7Cl_2N_5O_2S$: C, 38.39; H, 2.05; N, 20.35; S, 9.32. Found: C, 38.33; H, 2.00; N, 20.29; S, 9.40.EIMS calculated for $C_{11}H_7Cl_2N_5O_2S$ ($M^{+\bullet}$) 343.

2-Nitrobenzoic acid derivative of triazine (3i).

Mol.Wt: 372; Yellow solid, R_f 0.36; FTIR: 3421 (N-H), 1703 (C═O), 1592 (C═N), 1485 (NO_2), 1094 (S═O), 663 (C—Cl) cm^{-1}; ^1H NMR (300 MHz, DMSO-d_6): δ 11.33 (br s, 2H, N*H*), 8.43 (dd, *J* = 7.4, 2.0 Hz, 1H), 7.95 (dd, *J* = 7.5, 2.0 Hz, 1H), 7.84 (td, *J* = 7.5, 2.0 Hz, 1H), 7.72 (td, *J* = 7.4, 2.0 Hz, 1H). ^{13}C NMR (75 MHz, DMSO-d_6): δ 179.53 (C═S), 167.87 (C═O), 165.20 (C—Cl), 163.15 (C═N), 146.66-125.42 (Ar-*C*). Anal. Calcd for $C_{11}H_6Cl_2N_6O_3S$: C, 35.41; H, 1.62; N, 22.52; S, 8.59. Found: C, 35.36; H, 1.66; N, 22.48; S, 8.65.EIMS calculated for $C_{11}H_6Cl_2N_6O_3S$ ($M^{+\bullet}$) 372.

4-Nitrobenzoic acid derivative of triazine (3j).

Mol.Wt: 372; Yellow solid, R_f 0.31; FTIR: 3438 (N—H), 1715 (C═O), 1607 (C═N), 1480 (NO_2), 1071 (S═O), 651 (C—Cl) cm^{-1}; ^1H NMR (300 MHz, DMSO-d_6): δ 11.20 (br s, 2H, N*H*), 8.28 (d, *J* = 7.8 Hz, 2H), 7.96 (d, *J* = 7.8 Hz, 2H). ^{13}C NMR (75 MHz, DMSO-d_6): δ 176.92 (C═S), 167.34 (C═O), 165.75 (C—Cl), 163.15 (C═N), 148.40-123.99 (Ar—*C*). Anal. Calcd for $C_{11}H_6Cl_2N_6O_3S$: C, 35.41; H, 1.62; N, 22.52; S, 8.59. Found: C, 35.35; H, 1.67; N, 22.48; S, 8.64.EIMS calculated for $C_{11}H_6Cl_2N_6O_3S$ ($M^{+\bullet}$) 372.

4-Methylbenzoic acid derivative of triazine (3k).

Mol.Wt: 341; Light yellow solid, R_f 0.40; FTIR: 3460 (N-H), 1705 (C═O), 1598 (C═N), 1420 (C—H), 1080 (S═O). 650 (C—Cl) cm^{-1}; ^1H NMR (300 MHz, DMSO-d_6): δ 11.24 (br s, 2H, N*H*), 7.95 (d, *J* = 7.9 Hz, 2H), 7.38 (d, *J* = 7.9 Hz, 2H), 2.30 (s, 3H). ^{13}C NMR (75 MHz, DMSO-d_6): δ 175.71 (C═S), 168.55 (C═O), 165.75 (C-Cl), 163.15 (C═N), 140.36 to 128.32 (Ar—*C*), 21.42 (CH_3). Anal. Calcd for $C_{12}H_9Cl_2N_5OS$: C, 42.12; H, 2.65; N, 20.47; S, 9.37. Found: C, 42.06; H, 2.69; N, 20.40; S, 9.44.EIMS calculated for $C_{12}H_9Cl_2N_5OS$ ($M^{+\bullet}$) 341.

4-Methoxybenzoic acid derivative of triazine (3l).

Mol.Wt: 357; Light yellow solid, R_f 0.34; FTIR: 3413 (N—H), 1710 (C═O), 1598 (C═N), 1108 (C—O), 1067 (S═O), 658 (C—Cl) cm^{-1}; ^1H NMR (300 MHz, DMSO-d_6): δ 11.22 (br s, 1H, N*H*), 11.12 (br s, 1H, N*H*), 8.04 (d, *J* = 7.7 Hz, 2H), 7.06 (d, *J* = 7.7 Hz, 2H), 3.80 (s, 3H). ^{13}C NMR (75 MHz, DMSO-d_6): δ 176.62 (C═S), 1167.93 (C═O), 165.75 (C—Cl), 163.15 (C═N), 162.21-114.06 (Ar-C), 55.35 (O-CH_3). Anal. Calcd for $C_{12}H_9Cl_2N_5O_2S$: C, 40.24; H, 2.53; N, 19.55; S, 8.95. Found: C, 40.18; H, 2.58; N, 19.47; S, 9.02.EIMS calculated for $C_{12}H_9Cl_2N_5O_2S$ ($M^{+\bullet}$) 357.

Benzoic acid derivative of stilbene-triazine (5a).

Mol.Wt: 997.8; Light yellow solid, Yield 68%; R_f 0.21 FTIR: 3414 (N-H), 1708 (C═O), 1035 (S═O) cm^{-1}; ^1H NMR (300 MHz, DMSO-d_6): δ 11.14 (br s, 3H, N*H*), 7.91-7.21 (Ar-*H*), 7.09 (d, 1H, C*H*═C*H*); ^{13}C NMR (75 MHz, DMSO-d_6): δ 177.36 (*C*═S), 168.81 (*C*═O), 164.37 (*C*—Cl), 146.82-113.12 (Ar-*C*), 126.42 (*C*H═*C*H). Anal. Calcd for $C_{36}H_{24}Cl_2N_{12}Na_2O_8S_4$: C, 43.33; H, 2.42; N, 16.85; S, 12.85. Found: C, 43.41; H, 2.40; N, 16.79; S, 12.90. EIMS calculated for $C_{36}H_{24}Cl_2N_{12}Na_2O_8S_4$ ($M^{+\bullet}$) 997.

2-Hydroxy-3,4-dinitrobenzoic acid derivative of stilbene-triazine (5b).

Mol.Wt: 1209.8; Deep yellow solid, Yield 71%; R_f 0.19 FTIR: 3428 (N—H), 1703 (C═O), 1049 (S═O) cm^{-1}; ^1H NMR (300 MHz, DMSO-d_6): δ 11.15 (br s, 3H, N*H*),

8.28-7.63 (Ar-*H*), 7.09 (d, 1H, C*H*═C*H*), 5.13 (s, 1H, O*H*); ^{13}C NMR (75 MHz, DMSO-d_6): δ 177.15 (*C*═S), 167.08 (*C*═O), 165.65 (*C*—Cl), 159.27 (*C*—OH), 148.09 (*C*—NO_2), 139.95-108.30 (Ar—*C*), 126.21 (*C*H═*C*H). Anal. Calcd for $C_{36}H_{20}Cl_2N_{16}Na_2O_{18}S_4$: C, 35.74; H, 1.67; N, 18.52; S, 10.60. Found: C, 35.67; H, 1.62; N, 18.58; S, 10.51. EIMS calculated for $C_{36}H_{20}Cl_2N_{16}Na_2O_{18}S_4$ ($M^{+\bullet}$) 1209.

3,4,5-Trimethoxybenzoic acid derivative of stilbene-triazine (5c).

Mol.Wt: 1178; Light yellow solid, Yield 65%; R_f 0.20 FTIR: 3412 (N-H), 1709 (C═O), 1062 (S═O) cm^{-1}; ^{1}H NMR (300 MHz, DMSO-d_6): δ 11.32 (br s, 3H, N*H*), 8.70-7.80 (Ar-*H*), 7.09 (d, 1H, C*H*═C*H*), 3.75 (s, 9H, O*CH*$_3$); ^{13}C NMR (75 MHz, DMSO-d_6): δ 178.28 (*C*═S), 168.18 (*C*═O), 161.35 (*C*—Cl), 150.97-149.43 (*C*-OCH_3), 143.59-108.15 (Ar-*C*), 126.44 (*C*H═*C*H), 57.69-57.22 (O*C*H_3). Anal. Calcd for $C_{42}H_{36}Cl_2N_{12}Na_2O_{14}S_4$: C, 42.82; H, 3.08; N, 14.27; S, 10.89. Found: C, 42.73; H, 3.14; N, 14.32; S, 10.92. EIMS calculated for $C_{42}H_{36}Cl_2N_{12}Na_2O_{14}S_4$ ($M^{+\bullet}$) 1178.

2-Flouro-3-methoxy-4-bromobenzoic acid derivative of stilbene-triazine (5d).

Mol.Wt: 1251.6; Light yellow solid, Yield 75%; R_f 0.16 FTIR: 3441 (N—H), 1711 (C═O), 1072 (S═O) cm^{-1}; ^{1}H NMR (300 MHz, DMSO-d_6): δ 11.66 (br s, 3H, N*H*), 7.90-7.28 (Ar-*H*), 7.09 (d, 1H, C*H*═C*H*), 3.36 (s, 3H, O*CH*$_3$); ^{13}C NMR (75 MHz, DMSO-d_6): δ 177.97 (*C*═S), 168.53 (*C*═O), 160.11 (*C*—Cl), 152.02 (*C*—OCH_3), 148.51 (*C*—F), 136.30-105.26 (Ar—*C*), 111.67 (*C*—Br), 55.62 (O*C*H_3). Anal. Calcd for $C_{38}H_{24}Br_2Cl_2F_2N_{12}Na_2O_{10}S_4$: C, 36.47; H, 1.93; N, 13.43; S, 10.25. Found: C, 36.52; H, 1.99; N, 13.49; S, 10.19. EIMS calculated for $C_{38}H_{24}Br_2Cl_2F_2N_{12}Na_2O_{10}S_4$ ($M^{+\bullet}$) 1251.

3,5-Dihydroxybenzoic acid derivative of stilbene-triazine (5e).

Mol.Wt: 1061.8; Light yellow solid, Yield 70%; R_f 0.18 FTIR: 3398 (N-H), 1712 (C═O), 1077 (S═O) cm^{-1}; ^{1}H NMR (300 MHz, DMSO-d_6): δ 11.17 (br s, 3H, N*H*), 7.82-7.28 (Ar-*H*), 7.09 (d, 1H, C*H*═C*H*), 5.45 (s, 1H, O*H*), 5.39 (s, 1H, O*H*); ^{13}C NMR (75 MHz, DMSO-d_6): δ 177.84 (*C*═S), 168.05 (*C*═O), 163.10 (*C*—Cl), 161.31 (*C*—OH), 153.35-103.33 (Ar—*C*), 126.11 (*C*H ═ *C*H). Anal. Calcd for $C_{36}H_{24}Cl_2N_{12}Na_2O_{12}S_4$: C, 40.72; H, 2.28; N, 15.83; S, 12.08. Found: C, 40.66; H, 2.35; N, 15.78; S, 12.16. EIMS calculated for $C_{36}H_{24}Cl_2N_{12}Na_2O_{12}S_4$ ($M^{+\bullet}$) 1061.

2-Bromobenzoic acid derivative of stilbene-triazine (5f).

Mol.Wt: 1151.81; Light yellow solid, Yield 67%; R_f 0.23 FTIR: 3424 (N-H), 1710 (C═O), 1068 (S═O) cm^{-1}; ^{1}H NMR (300 MHz, DMSO-d_6): δ 11.21 (br s, 3H, N*H*), 7.68-6.50 (Ar-*H*), 7.09 (d, 1H, C*H*═C*H*); ^{13}C NMR (75 MHz, DMSO-d_6): δ 178.66 (*C*═S), 171.51 (*C*═O), 168.26 (*C*—Cl), 150.41-113.17 (Ar-*C*), 126.47 (*C*H═*C*H), 120.18 (*C*—Br). Anal. Calcd for $C_{36}H_{22}Br_2Cl_2N_{12}Na_2O_8S_4$: C, 37.42; H, 1.92; N, 14.54; S, 11.10. Found: C, 37.55; H, 1.96; N, 14.49; S, 11.21. EIMS calculated for $C_{36}H_{22}Br_2Cl_2N_{12}Na_2O_8S_4$ ($M^{+\bullet}$) 1155.

2-Methylbenzoic acid derivative of stilbene-triazine (5g).

Mol.Wt: 1025.8; Light yellow solid, Yield 69%; R_f 0.17 FTIR: 3405 (N—H), 1705 (C═O), 1051 (S═O) cm^{-1}; ^{1}H NMR (300 MHz, DMSO-d_6): δ 12.02 (br s, 3H, N*H*), 7.88-7.48 (Ar—*H*), 7.09 (d, 1H, C*H*═C*H*), 2.92 (s, 3H, C*H*$_3$); ^{13}C NMR (75 MHz, DMSO-d_6): δ 178.14 (*C*═S), 170.78 (*C*═O), 163.14 (*C*—Cl), 154.13-102.10 (Ar—*C*), 136.56 (*C*—CH_3), 126.13 (*C*H═*C*H), 18.29 (CH_3). Anal. Calcd for $C_{38}H_{28}Cl_2N_{12}Na_2O_8S_4$: C, 44.49; H, 2.75; N, 16.38; S, 12.50. Found: C, 44.53; H, 2.80; N, 16.44; S, 12.45. EIMS calculated for $C_{38}H_{28}Cl_2N_{12}Na_2O_8S_4$ ($M^{+\bullet}$) 1025.

2-Hydroxybenzoic acid derivative of stilbene-triazine (5h).

Mol.Wt: 1029.8; Light yellow solid, Yield 72%; R_f 0.22 FTIR: 3372 (N—H), 1714 (C═O), 1075 (S═O) cm^{-1}; ^{1}H NMR (300 MHz, DMSO-d_6): δ 11.24 (br s, 3H, N*H*), 7.90-7.22 (Ar-*H*), 7.09 (d, 1H, C*H*═C*H*), 5.82 (s, 1H, O*H*); ^{13}C NMR (75 MHz, DMSO-d_6): δ 176.75 (*C*═S), 168.26 (*C*═O), 160.14 (*C*—OH), 158.41 (*C*—Cl), 146.93-110.12 (Ar—*C*), 126.30 (*C*H═*C*H). Anal. Calcd for $C_{36}H_{24}Cl_2N_{12}Na_2O_{10}S_4$: C, 41.99; H, 2.35; N, 16.32; S, 12.45. Found: C, 41.89; H, 2.39; N, 16.28; S, 12.39. EIMS calculated for $C_{36}H_{24}Cl_2N_{12}Na_2O_{10}S_4$ ($M^{+\bullet}$) 1029.

2-Nitrobenzoic acid derivative of stilbene-triazine (5i).

Mol.Wt: 1087.8; Yellow solid, Yield 78%; R_f 0.19 FTIR: 3415 (N-H), 1702 (C═O), 1098 (S═O) cm^{-1}; ^{1}H NMR (300 MHz, DMSO-d_6): δ 11.80 (br s, 3H, N*H*), 7.78-7.23 (Ar-*H*), 7.09 (d, 1H, C*H*═C*H*); ^{13}C NMR (75 MHz, DMSO-d_6): δ 178.02 (*C*═S), 168.67 (*C*═O), 167.95 (*C*-Cl), 148.80 (C-NO_2), 145.00-105.97 (Ar-*C*), 126.10 (*C*H═*C*H). Anal. Calcd for $C_{36}H_{22}Cl_2N_{14}Na_2O_{12}S_4$: C, 39.75; H, 2.04; N, 18.03; S, 11.79. Found: C, 39.70; H, 2.11; N, 18.23; S, 11.84. EIMS calculated for $C_{36}H_{22}Cl_2N_{14}Na_2O_{12}S_4$ ($M^{+\bullet}$) 1087.

4-Nitrobenzoic acid derivative of stilbene-triazine (5j).

Mol.Wt: 1087.8; Yellow solid, Yield 58%; R_f 0.21 FTIR: 3430 (N-H), 1701 (C═O), 1079 (S═O) cm^{-1}; ^{1}H NMR (300 MHz, DMSO-d_6): δ 11.31 (br s, 3H, N*H*), 8.04-7.84 (Ar-*H*), 7.09 (d, 1H, C*H*═C*H*); ^{13}C NMR (75 MHz, DMSO-d_6): δ 176.33 (*C*═S), 169.87 (*C*═O), 168.20 (*C*-Cl), 151.81 (*C*-NO_2), 138.44-105.24 (Ar-*C*), 126.37 (*C*H═*C*H). Anal. Calcd for $C_{36}H_{22}Cl_2N_{14}Na_2O_{12}S_4$: C, 39.75; H, 2.04; N, 18.03; S, 11.79. Found: C, 39.81; H, 2.12; N, 18.26; S, 11.86. EIMS calculated for $C_{36}H_{22}Cl_2N_{14}Na_2O_{12}S_4$ ($M^{+\bullet}$) 1088.

4-Methylbenzoic acid derivative of stilbene-triazine (5 k).

Mol.Wt: 1025.8; Light yellow solid, Yield 79%; R_f 0.15 FTIR: 3465 (N-H), 1706 (C═O), 1085 (S═O) cm^{-1}; ^{1}H

NMR (300 MHz, DMSO-d_6): δ 11.36 (br s, 3H, N*H*), 7.70-7.14 (Ar-*H*), 7.09 (d, 1H, C*H*═C*H*), 2.79 (s, 3H, CH_3); ^{13}C NMR (75 MHz, DMSO-d_6): δ 178.53 (*C*═S), 169.16 (*C*═O), 166.20 (*C*—Cl), 163.33-100.19 (Ar—*C*), 143.30 (*C*—CH_3), 126.63 (*C*H═*C*H), 24.32 (*C*H_3). Anal. Calcd for $C_{38}H_{28}Cl_2N_{12}Na_2O_8S_4$: C, 44.49; H, 2.75; N, 16.38; S, 12.50. Found: C, 44.40; H, 2.67; N, 16.42; S, 12.59. EIMS calculated for $C_{38}H_{28}Cl_2N_{12}Na_2O_8S_4$ ($M^{+\bullet}$) 1025.

4-Methoxybenzoic acid derivative of stilbene-triazine (5 L).

Mol.Wt: 1057.8; Light yellow solid, Yield 67%; R_f 0.24 FTIR: 3418 (N-H), 1707 (C═O), 1069 (S═O) cm^{-1}; ^{1}H NMR (300 MHz, DMSO-d_6): δ 11.12 (br s, 3H, N*H*), 7.94-7.36 (Ar-*H*), 7.09 (d, 1H, C*H*═C*H*), 3.70 (s, 3H, OCH_3); ^{13}C NMR (75 MHz, DMSO-d_6): δ 176.43 (*C*═S), 164.24 (*C*═O), 159.64 (*C*-OCH_3), 153.68 (*C*-Cl), 145.18-110.60 (Ar-*C*), 126.39 (*C*H═*C*H), 54.97 (O*C*H_3). Anal. Calcd for $C_{38}H_{28}Cl_2N_{12}Na_2O_{10}S_4$: C, 43.14; H, 2.67; N, 15.89; S, 12.12. Found: C, 43.20; H, 2.58; Cl, 6.77; N, 15.95; S, 12.07. EIMS calculated for $C_{38}H_{28}Cl_2N_{12}Na_2O_{10}S_4$ ($M^{+\bullet}$) 1057.

3.3 | LYP inhibition assay

LYP assays were performed in black 96-well microplates in a total volume of 100 µL using Molecular Devices Spectramax M5 plate reader. Unless otherwise noted, all solutions were prepared using a Bis-Tris (50 mM, pH 6.5) buffer containing 100 mM NaCl and 0.01% Brij35. Inhibitor compound and TCEP solutions were prepared using DMSO. Each well contained 3.58 nM LYP, 100 µM tris (2-carboxyethyl)phosphine (TCEP), 5 µM 6,8-difluoro-4-methylumbelliferyl phosphate (DiFMUP), and either 100 µM of inhibitor (initial screen), 1-400 µM inhibitor (IC_{50} determination), or DMSO, resulting in a final DMSO concentration of 6.1% (v/v). Prior to testing, 35.8 nM LYP was activated by incubation with 1 mM TCEP on ice for 30 minutes. After addition to an appropriate amount of buffer, inhibitor compounds were added and allowed to incubate for 30 minutes at room temperature. Reactions were initiated by addition of DiFMUP to each. The enzymatic turnover of DiFMUP to the fluorescent compound DiFMU was used to determine enzyme activity, with fluorescence measured every 60 seconds over a 30 minute period (λex = 350 nm, λem = 455 nm). Percent inhibition was calculated by averaging the initial enzyme activities for each inhibitor and normalizing them against a set of DMSO control wells. The IC_{50} value of each inhibitor was determined using plots of initial enzyme activity against inhibitor concentration. Initial screen experiments were run in duplicate while IC_{50} testing was run in triplicates.

3.4 | Computational modeling study

Crystal structure of LYP protein was obtained from RCSB (PDB entry 3OLR)[32,33] and chain A was utilized for modeling purpose. The crystal structure was (resolution 2.5 Å) solved in complex with phosphotyrosine residue, thereby providing a suitable starting point for computational studies. The protein was prepared by adding missing hydrogens and optimized using Protein Prep module of the Schrodinger program.[34,35] A grid was generated for docking purposes by placing a box of length 20 Å in each XYZ direction centering at the phosphotyrosine residue. The ligands (compound **5a**, **5d**, **5e**, **5g**, **5k**, & **5l**) were prepared using ligprep module of the Schrodinger program. Glide standard precision (Glide-SP) module was used for docking simulations.[35]

4 | CONCLUSIONS

A series of molecules incorporating thiourea- stilbene-triazines moieties (**5a-i**) was synthesized as a new entry to protein tyrosine phosphatase LYP inhibitors. To ascertain the possible influence of inhibitory potential of compounds **5a** to **5l** molecular docking was performed. On the bases of docking computations, compound **5k** and **5l** showed good binding mode. Thus, we suggest that the electrostatic and hydrophobic interactions exist between the targets and compounds **5l** are well corroborated by the experimental data. Docking simulation also elucidated the valuable information to understand the binding pattern and inhibitory potential and contribute to the molecular design of novel synthetic inhibitors to inhibit the activities of LYP to quite a good level. These results further demonstrate that the compound **5l** can serve as the potential candidate for hit to lead generation and design of novel antibacterial and anti-fungal agents.

ACKNOWLEDGEMENTS

We are grateful to Dr. Amy M. Barrios at the University of Utah, College of Pharmacy for assistance with the enzyme inhibition assays.

ORCID

Aamer Saeed https://orcid.org/0000-0002-7112-9296

REFERENCES

[1] I. Orhan, F. Tosun, B. Şener, *Zeitschrift für Natur. C.* **2008**, *63* (5–6), 366.

[2] O. Bekircana, M. Küxükb, B. Kahvecic, S. Kolayl, *Arch. Pharm. Chem. Life Sci.* **2005**, *338*, 365.

[3] Z. Nie, C. Perretta, P. Erickson, S. L. Margosiak, J. Averill, A. Almassy, R. Chu, *Bioorg. Med. Chem. Lett.* **2008**, *18*, 619.

[4] P. Mullick, A. K. Suroor, T. Begum, S. Verma, D. Kaushik, O. Alam, *Acta Polon. Pharma. Drug Res.* **2009**, *66*(4), 379.
[5] B. K. K. Pankaj, H. C. Nisha, K. S. Dhaval, P. P. Dharmendra, H. P. Govindraj, V. M, *ARKIVOC,* **2009**, *2009*(11), 326.
[6] A. S. R. L. Jennings, R. T. Russell, M. G. N. Hallett, D. J. Street, L. J. Castro, J. L. Atack, J. R. Cook, S. M. Lincoln, R. Stanley, J. Smith, A. J. Reynolds, D. S. Sohal, B. Pike, A. Marshall, G. R. Wafford, K. A. Tye, S. J, *Bioorg. Med. Chem. Lett.* **2006**, *16*, 1477.
[7] Z. El-Gendy, Z. Morsy, J. M. Allimony, H. A. Abdel-Monem, W. R. Abdel-Rahman, *Phosphorus, Sulfur, and Silicon* **2003**, *178*, 2055.
[8] A. K. Mansour, M. E. Mohga, S. A. M. K. Nasser, *Nucle. Nucle. Nucleic Acids.* **2003**, *22*(1), 21.
[9] F. Sączewski, A. Bułakowska, P. Bednarski, R. Grunert, *Eur. J. Med. Chem.* **2006**, *41*(2), 219.
[10] G. Ivo, *Dyes. Pigm.* **1995**, *29*(2), 155.
[11] Y. Wang, W. You, Y. Song, X. Li, D. Qiu, M. Cheng, F. Shi, *J. Mater. Chem. B.* **2017**, *5*(2), 375.
[12] G. Ivo, P. Tzvetanka, *Die Ang. Makromole. Chem.* **1998**, *263*, 14.
[13] G. Ivo, P. Tzvetanka, *Dyes. Pigm.* **2000**, *44*, 175.
[14] G. Ivo, *J. Photochem. Photobio A: Chem.* **2000**, *135*(1), 41.
[15] M. Wan, S. Zhou, P. Jiao, C. Cao, J. Guo, *J. Fluoresc.* **2013**, *23* (5), 1099.
[16] T. Mustelin, T. Vang, N. Bottini, *Nat. Rev. Immunol.* **2005**, *5* (1), 43.
[17] T. Hunter, *Curr. Opin. Cell Biol.,* **2009**, *21*(2), 140.
[18] N. Bottini, E. J. Peterson, *Annu. Rev. Immunol.* **2014**, *32*, 83.
[19] V. Orru, S. J. Tsai, B. Rueda, E. Fiorillo, S. M. Stanford, J. Dasgupta, J. Hartiala, L. Zhao, N. Ortego-Centeno, S. D'Alfonso, F. C. W. Arnett, H. Gonzalez-Gay, M. Tsao, B. P. Pons-Estel, B. Alarcon-Riquelme, M. E. He, Y. Zhang, Z.-Y. Allayee, H. Chen, X. S. Martin, J. Bottini, *Humn. Genet* **2008**, *18*(3), 569.
[20] J. Golenbiewski,, R.T. Keenan, *Rheumatol Ther.* **2019**, *6*, 179.
[21] L.-M. E.-P. Diaz-Gallo, L. Fransen, K. Gómez-García, M. van Sommeren, S. Cardeña, C. Rodrigo, L. Mendoza, J. L. Taxonera, C. Nieto, A. Alcain, G. Cueto, I. López-Nevot, M. Bottini, N. Barclay, M. L. Crusius, B. J. van Bodegraven, A. Wijmenga, C. Ponsioen, C. Y. Gearry, R. B. Roberts, R. L. Weersma, R. K. Urcelay, E. Merriman, T. R. Alizadeh, B. Z, *J. Inflamm. Bowel Dis.* **2011**, *17*(11), 2287.
[22] N. Bottini, L. Musumeci, A. Alonso, S. Rahmouni, K. Nika, M. Rostamkhani, J. MacMurray, G. F. Meloni, P. Lucarelli, M. Pellecchia, G. S. Eisenbarth, D. Comings, *Nat. Genet.* **2004**, *36* (4), 337.
[23] L. M. Chow, M. Fournel, D. Davidson, A. Veillette, *Nature* **1993**, *365*(6442), 156.
[24] J. Du, Y. Qiao, L. Sun, X. Wang, *Current drug targ.* **2014**, *15* (3), 335.
[25] A. B. C. Begovich, V. E. Honigberg, L. Schrodi, S. J. Chokkalingam, P. Alexander, H. C. Ardlie, K. G. Huang, Q. Smith, M. Spoerke, J. M. Conn, M. T. Chang, M. Chang, S. Y. Saiki, R. K. Catanese, J. J. Leong, D. U. Garcia, V. E. McAllister, L. B. Jeffery, D. Lee, T. Batliwalla, F. Remmers, E. Criswell, L. Seldin, M. F. Kastner, D. L. Amos, C. I. Sninsky, J. J. Gregersen, P. K, *Am. J. Hum. Genet.* **2004**, *75*(2), 330.
[26] C. Kyogoku, C. D. Langefeld, W. Ortmann, A. Lee, S. Selby, V. E. H. Carlton, M. Chang, P. Ramos, E. C. Baechler, F. M. Batliwalla, J. Novitzke, A. H. Williams, C. Gillett, P. Rodine, R. R. Graham, K. G. Ardlie, P. M. Gaffney, K. L. Moser, M. Petri, A. B. Begovich, P. K. Gregersen, T. W. Behrens, *Am. J. Hum. Genet.* **2004**, *75*(3), 504.
[27] M. R. Velaga, V. Wilson, C. E. Jennings, C. J. Owen, S. Herington, P. T. Donaldson, S. G. Ball, R. James, R. Quinton, P. Perros, S. H. S. Pearce, *J.Clinic. Endo. Metabol.* **2004**, *89*(11), 5862.
[28] Y. He, S. Liu, A. Menon, S. Stanford, E. Oppong, A. M. Gunawan, L. Wu, D. J. Wu, A. M. Barrios, N. Bottini, A. C. Cato, Z. Y. Zhang, *J Med Chem.* **2013**, *56*(12), 49904008
[29] S. M. Stanford, D. Krishnamurthy, M. D. Falk, R. Messina, B. Debnath, S. Li, X. Yu, *J. Med. Chem.* **2011**, *54*(6), 1640.
[30] R. Kulkarni, N. Vellore, M. R. Bliss, S. M. Stanford, M. D. Falk, N. Bottini, R. Baron, A. M. Barrios, *ChemBioChem* **2013**, *14*(13), 16401647
[31] M. B. Soellner, K. A. Rawls, C. Grundner, A Tom, A. E. Jonathan, *J. Am. Chem. Soc.* **2007**, *129*(31), 9613.
[32] X. Yu, J.-P. Sun, S. Zhang, Z.-Y. Zhang. PTPN22 in complex with consensus phospho-tyrosine peptide. HYDROLASE, **2010**, DOI: 10.2210/pdb3OLR/pdb
[33] H. Xuben, K. Li, X. Yu, J. Sun, H. Fang, *J Chem inf Model*. **2015**, *55*(9), 1973.
[34] Schrödinger Release 2016-4: Schrödinger Suite 2016-4 Protein Preparation Wizard; Schrödinger, LLC, New York, NY, **2016**.
[35] Schrödinger Release 2016-4: Schrödinger Suite 2016-4 Ligand Docking protocol; Glide, Schrödinger, LLC, New York, NY, **2016**.

SUPPORTING INFORMATION

Additional supporting information may be found online in the Supporting Information section at the end of this article.

How to cite this article: Batool I, Jabeen F, Vellore NA, Shabir G, Saeed A. Identification of novel thiourea-stilbene-triazine conjugates as persuasive lymphoid tyrosine phosphatase inhibitors. *J Heterocyclic Chem*. 2020;1–12. https://doi.org/10.1002/jhet.4060